Biosensors and Bioelectronics 66 (2015) 103–108

Contents lists available at ScienceDirect

Biosensors and Bioelectronics

journal homepage: www.elsevier.com/locate/bios

Cu^{2+} modulated silver nanoclusters as an on–off–on fluorescence probe for the selective detection of L-histidine

Xuyue Zheng, Tianming Yao*, Ying Zhu, Shuo Shi*

Department of Chemistry, Tongji University, Shanghai 200092, China

ARTICLE INFO

Article history:
Received 25 July 2014
Received in revised form
23 October 2014
Accepted 9 November 2014
Available online 11 November 2014

Keywords:
Silver nanoclusters
DNA biosensor
Fluorescence
L-histidine

ABSTRACT

In the present study, a new strategy based on Cu^{2+} mediated DNA-templated silver nanoclusters (DNA-Ag NCs) was developed, as a label-free, on–off–on fluorescent probe for the detection of L-histidine. Eight synthesized DNA oligonucleotides (D1–D8) were experimentally tested, and D5-Ag NCs was finally selected for L-histidine detection due to its best fluorescent properties. The fluorescence emission of D5-Ag NCs could be quenched by Cu^{2+} via electron or energy transfer. Upon addition of L-histidine, the chelation between Cu^{2+} and the imidazole group of L-histidine leads to Cu^{2+} liberation from D5-Ag NCs, and subsequently results in a dramatic fluorescence enhancement of the probe. The method displayed a good selectivity toward L-histidine over all the other amino acids, with a linear relationship in the range of 0.20–80 μM, and a limit of detection (LOD) of 4.3 nM. The strategy was also successfully applied to detect L-histidine in diluted human urine, exhibiting great opportunities for practical application in biological system.

1. Introduction

L-histidine, one of the 20 naturally occurring amino acids in protein, can usually be found in catalytic sites in enzymes. Due to its aromatic nitrogen- heterocyclic imidazole side chain, it plays a very crucial role in many biological systems, for example, to control metal transport in biologically important bases (Li et al., 2004), and to minimize internal bleeding from microtrauma (Li et al., 2011). The persistent deficiency of L-histidine was reported to be associated with Friedreich ataxia, epilepsy, Parkinson's disease, and the failure of normal erythropoiesis development (Li et al., 2013). On the other hand, overexpression of L-histidine in physiological fluids, such as serum and urine, could induce metabolic disorders or histidinemia (Oliveira et al., 2013). Therefore, the rapid, selective and quantificational detection of L-histidine is of great importance for biological applications including both pharmaceutical research and clinical treatment.

Up to date, there have emerged lots of L-histidine detection methods, including capillary electrophoresis (Zhang and Sun, 2004; Zhou et al., 2010), liquid chromatography (Tateda et al., 1998), electrochemistry (Chen et al., 2014, 2012; Huang et al., 2012; Li et al., 2011; Liang et al., 2011), colorimetry (Sun et al., 2012; Zhang et al., 2012b), spectrofluorimetry (Elbaz et al., 2008; Folmer-Andersen et al., 2005; Fu et al., 2013; He et al., 2013, 2012; Huang et al., 2012; Kong et al., 2011; Li et al., 2013; Oliveira et al., 2013; Wu and Yan, 2010; Zhou et al., 2014). These methods, while most successful, some of them still suffer drawbacks, including cumbersome optical equipment, expensive robotic facilities and complicated operation procedures, tedious pre-treatment of the biological sample, or lower limit detection etc. Recently, as a useful analytical technology, fluorescent biosensors have been extensively employed as they could provide simple operation procedures, high sensitivity, long linear range, and low detection limit, etc. Therefore, there are still necessary and importance to explore facile and low-cost fluorescence sensors for L-histidine detection.

Fluorescent metal nanoclusters (NCs) are composed of several to roughly hundreds of atoms of noble metal. Their sizes are comparable to the Fermi wavelength of electrons, exhibiting molecule-like properties including discrete energy levels and size-dependent fluorescence (Shang et al., 2011). Among various metallic NCs, Au and Ag nanoclusters are the most popular sensing materials, because of their strong fluorescence properties, stability, and biocompatibility. Song et al. have developed Ni^{2+}-modified gold nanoclusters complex for the detection of histidine (He et al., 2012). Compared to gold nanoclusters, silver nanoclusters are brighter and can be easily synthesized with different synthetic strategies (Han and Wang, 2012; Liu, 2014; Zhang and Wang, 2014; Zheng et al., 2007). Noteworthily it has been demonstrated that DNA with different sequences have distinct binding capabilities toward Ag^{+} ions, therefore, DNA templates can regulate the size of synthetic Ag NCs, and subsequently determine their fluorescence

* Corresponding authors. Fax: +86 21 6598 2287.
E-mail addresses: tmyao@tongji.edu.cn (T. Yao), shishuo@tongji.edu.cn (S. Shi).

http://dx.doi.org/10.1016/j.bios.2014.11.013
0956-5663/

quantum yield (QY) as well as emission wavelength (Richards et al., 2008; Sharma et al., 2010; Yeh et al., 2010). The versatility of DNA-templated silver nanoclusters (DNA-Ag NCs) has provoked interest of researchers from different fields. Up to now, it has been reported that DNA-Ag NCs can be applied to biological imaging (Ai et al., 2012; Li et al., 2012a; Yin et al., 2012), as well as fluorescent sensors of various analytes including metal ions (Lan et al., 2010; Yu and Wang, 2011; Zhang et al., 2012a), small biomolecules (Han and Wang, 2011; Huang et al., 2011; Zhang et al., 2013c), proteins (Li et al., 2012b; Liu et al., 2012; Sharma et al., 2011) and nucleic acids (Guo et al., 2010; Liu et al., 2013; Ma et al., 2011; Yeh et al., 2010, 2012; Zhang et al., 2013a), based on the fluorescence quenching or increasing effect.

Herein to seek further application of DNA-Ag NCs, we developed a label-free fluorescent probe for the detection of L-histidine. As the Ag NCs templates, eight DNA strands with different length and sequence (D1–D8) were experimentally tested, and the best one (D5) was finally selected due to its best fluorescent properties. The fluorescence emission of D5-Ag NCs could be quenched by Cu^{2+} via electron or energy transfer. The quenching ability of Cu^{2+} on D5-Ag NCs fluorescence was investigated. Upon addition of L-histidine, the strong chelation between Cu^{2+} and the imidazole group of L-histidine leads to Cu^{2+} liberation from D5-Ag NCs, and subsequently results in a dramatic fluorescence enhancement of the probe. In addition to imidazole ring of L-histidine, the thiol group of cysteine can also interact with Cu^{2+}. In this work, we successfully eliminated the interference of cysteine by introducing N-ethylmaleimide (NEM) which was widely used as a alkylating agent for the biologically important thiol group (Li et al., 2013). The method displayed a good selectivity toward L-histidine over all the other amino acids. And the practicality of the method was also validated for the analysis of human urine samples. Consequently, our work will give not only a useful strategy for highly selective detection of L-histidine, but also a deeper understanding about the specific interaction of Cu^{2+}, L-histidine and DNA-Ag NCs.

2. Experimental

2.1. Materials

DNA sequences (HPLC purified) used in this work are listed as follows: D1: 5′-CCC CCC CCC CCC-3′; D2: 5′-AAT TCC CCC CCC CAA TT-3′; D3: 5′-CCC TTC CTT CCT TCC AAC CAA CCC-3′; D4: 5′-CCC TTA ATC CCC-3′; D5: 5′-GGC AGG TTG GGG TGA CTA AAA ACC CTT AAT CCC C-3′; D6: 5′-AGT CCG TGG TAG GGC AGG TTG GGG TGA CTA AAA ACC CTT AAT CCC C-3′; D7: 5′-ACC CGA ACC TGG GCT ACC ACC CTT AAT CCC C-3′; D8: 5′-ATC CTC CCA CCG GCC CTC CCA CCA TAA AAA CCC TTA ATC CCC-3′. All of the synthesized oligonucleotides were purchased from Shanghai Sangon Biotechnology Co. Ltd. (Shanghai, China). All the other chemicals are at least of analytical reagent grade, purchased from Aladdin Ltd. (Shanghai, China) and Sinopharm Chemical Reagent Co. Ltd. (Shanghai, China), and used directly without further purification. The stock solution of NEM (50 mM) was prepared in dimethyl sulfoxide (DMSO) and stored in darkness at 4 °C before use. Phosphate buffer solution (20 mM PB) was used to control the acidity of the reaction solution. The fresh stock solutions of other chemicals were prepared in the triple distilled water.

2.2. Instruments

Fluorescence spectra were recorded at room temperature via an F-7000 fluorescence spectrophotometer (Hitachi Ltd., Japan) in a 1.0 cm path length quartz cuvette. The slot widths for both excitation and emission were fixed at 10 nm. A Perkin-Elmer Lambda Bio 40 UV/vis Spectrophotometer (Perkin-Elmer, USA) was used to measure the absorption spectra of DNA-Ag NCs in the range of 200–700 nm. The average size of the DNA-Ag NCs was determined by TEM images using a JEOL JEM-2100 high resolution TEM instrument. The fluorescence lifetime was measured by Time-Correlated Single Photon Counting (TCSPC), which is based on the detection of single photons of a periodical light signal. A 2×10^7 Hz 405 nm pico-second (ps) laser (Edinburgh Instruments, EPL405) was used for the excitation. The fluorescence decay courses was measured by a PMT (Hamamatsu, R928P) with a band-pass filter of 550–620 nm in the TCSPC (Edinburgh Instruments, TCC900).

2.3. Synthesis of DNA-Ag NCs

DNA-Ag NCs were prepared according to the literature with a slight modification (Zhang et al., 2013c). Briefly, 30 μL of DNA solution (100 μM, in 20 mM PB buffer, pH 6.6), 10 μL of $AgNO_3$ solution (18 mM, in distilled water), and 950 μL PB buffer (20 mM, pH 6.6) were placed in a small glass vessel, mixed under vigorously stirring by the magnetic stirring apparatus for 5 min and then incubated at room temperature in dark for 20 min. Afterwards, 10 μL of $NaBH_4$ solution (18 mM, freshly prepared in ice ultrapure water) was quickly added, thoroughly mixed, and then kept in dark at 4 °C for more than 5 h. Along with the reduction of Ag^+ ions, highly fluorescent DNA-Ag NCs were produced. For simplicity, the concentration of the as-prepared DNA-Ag NCs was denoted as "3.0 μM", according to the amount of DNA introduced into the system (Zhang et al., 2012a).

2.4. Fluorescence lifetime of DNA-Ag NCs

The obtained decay curves can be fitted with multi-exponential decay as described in Formula (1).

$$I(t) = \sum_{i=1}^{n} \alpha_i \exp\left(-\frac{t}{\tau_i}\right) \quad (1)$$

Where τ_i and α_i represent the decay constant and amplitude of each exponential component, respectively. The average lifetime (τ_{ave}) can be obtained according to Formula (2) (Xu et al., 2014)

$$\tau_{ave} = \frac{\sum_{i=1}^{n} \alpha_i \tau_i^2}{\sum_{i=1}^{n} \alpha_i \tau_i} \quad (2)$$

With the 3–5 times measurements, the τ_{ave} of DNA-Ag NCs (D1–D8) in different templates were obtained as shown in Fig. S1 and Table S1.

2.5. Fluorescence assay of L-histidine

For L-histidine detection, 40 μL of Cu^{2+} (10 μM, in 20 mM PB) were premixed with different amount of L-histidine in 910 μL phosphate buffer (20 mM, pH 7.4), and incubated for 30 min. Then, 50 μL of DNA-Ag NCs (3 μM, in 20 mM PB) were added into the mixture. To guarantee a completed reaction, the mixture was incubated for another 30 min. The final volume of each sample was 1 mL in 20 mM phosphate buffer, and the final concentrations of DNA-Ag NCs and Cu^{2+} were 150 nM and 400 nM, respectively. The fluorescent intensity was recorded at room temperature, on Hitachi F-7000 spectrophotometer with both the excitation and emission slot widths at 10 nm.

2.6. Selective and competitive detection of L-histidine

To investigate whether the other amino acids could interfere with the detection of L-histidine, the selectivity and competition of the fluorescence assay were studied in detail. And in order to

further differentiate L-histidine from cysteine, the samples which contained cysteine were pre-incubated with 50 μL of 10 mM NEM for 40 min before the Cu^{2+} (400 nM) and DNA-Ag NCs (150 nM) addition.

2.7. Analysis of L-histidine in urine samples

Human urine samples were collected from healthy adult volunteers in the morning. In order to eliminate potential interferences of biothiols in human urine, NEM was introduced to blocked biothiols. 250 μL of urine was vigorously mixed with 50 μL NEM (50 mM), then diluted 100 times and incubated for 20 min at room temperature before the following detection procedures. No other pretreatments were done for the detection of the real samples.

3. Results and discussion

3.1. Optimization and characterization of DNA-Ag NCs

Oligonucleotide-stabilized Ag nanoclusters have outstanding fluorescence and photophysical properties, compared with the conventional small-molecule dyes and quantum dots (QDs) (Cao et al., 2014; Yao et al., 2012). The fluorescence emission bands of these fluorophores can be tuned throughout the visible and near-IR range simply by varying oligonucleotide length and sequence (Lan et al., 2011a; Richards et al., 2008). Furthermore, the low toxicity and good biocompatibility of these fluorescent DNA-Ag NCs facilitate their application as environmentally-friendly and biocompatible fluorescence probes in optical sensor design. On the basis of these findings, we selected a series of DNA strands with different sequences and lengths to synthesize the bright DNA-Ag NCs (Guo et al., 2013; Han and Wang, 2011; Lan et al., 2011a; Richards et al., 2008; Sharma et al., 2012, 2010; Zhang and Ye, 2011; Zhang et al., 2013c; Zhou et al., 2014). DNA-Ag NCs (D1–D8) were prepared based on the previously reported method with a slight modification, 100 μM solution of DNA was mixed with $AgNO_3$ by the molar ratio of 1:6 for 25 min, then reduced by $NaBH_4$ to form DNA-Ag NCs (Zhang et al., 2013b). The distinct fluorescence properties of the resulted DNA-Ag NCs (D1–D8) are shown in Table S1 and Fig. S1, and their quenching effects for Cu^{2+} are shown in Fig. S2. Compared with the other DNA templates, D5-Ag NCs has higher quantum yield (QY>50%), longer fluorescence lifetime (4.57 ns). Also, its fluorescence intensity, as well as binding capability toward Cu^{2+}, is most suitable for the construction of fluorescence probe, thus D5-Ag NCs is selected for the further studies.

The optical properties of D5-Ag NCs were firstly characterized by UV/vis absorption spectrophotometer. The peak around 600 nm was the characteristic absorption of D5-Ag NC (Fig. S3a), while the peak at about 400 nm was the absorption of Ag nanoparticles (Ag NPs), (Kundu, 2013; Molotsky et al., 2010; Sakr et al., 2014; Sinha et al., 2014), the small amount of Ag NPs in the system had been proved to have little impact on the fluorescence behavior of DNA-Ag NCs (Guo et al., 2010; Ma et al., 2011; Zhang et al., 2013a, 2013b; Zhang and Ye, 2011). High resolution transmission electron microscopy (TEM) was further used to characterize the morphology of D5-Ag NCs, Fig. S3b showed that the average size of D5-Ag NCs was about 2 nm, which was consistent with the previous reports (Richards et al., 2008; Zhang et al., 2013b, 2013c).

3.2. Mechanism of the on–off–on fluorescence detection of L-histidine

As illustrated in Scheme 1, D5-Ag NCs with strong fluorescence emission was eventually obtained by us through selecting a particular sequence of oligonucleotide. In the presence of Cu^{2+}, the fluorescence of Ag NCs could be quenched (turn-off) via electron or energy transfer due to the specific interaction between Cu^{2+} and DNA (Zhang et al., 2013c). On the other hand, the imidazole group of L-histidine could tightly coordinate with Cu^{2+} to form a 2:1 His/Cu^{2+} complex (Folmer-Andersen et al., 2005). Upon addition of L-histidine, the interaction between Cu^{2+} and D5-Ag NCs would be weaken by the competitive coordination of imidazole group, and part of Cu^{2+} could be taken away from the D5-Ag NCs/Cu^{2+} complex, then the fluorescence of D5-Ag NCs would be dramatically enhanced. Thus, the detection of L-histidine could be realized based on the fluorescent response to the presence of L-histidine. As shown in Fig. 1, the as-prepared D5-Ag NCs showed a very strong fluorescence emission peak upon being excited at the 585 nm. When Cu^{2+} was mixed with D5-Ag NCs, the fluorescence intensity was decreased sharply, indicating that Cu^{2+} could effectively quench the fluorescence of D5-Ag NCs. However, upon addition of L-histidine, the fluorescence increased obviously. These results were conformity with the previously assumptive mechanism, and Cu^{2+} -modulated DNA-Ag NCs could be used as the fluorescence probe for the detection of L-histidine.

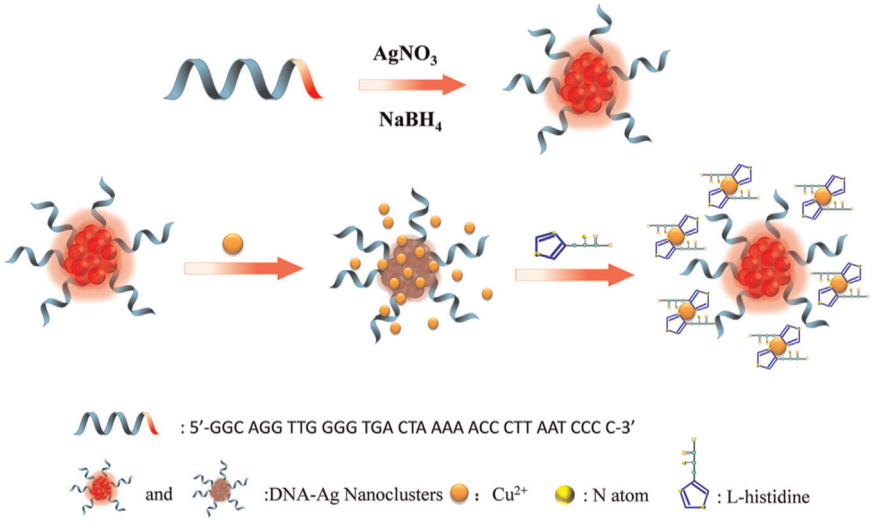

Scheme 1. Schematic illustration of the fluorescence sensor for the detection of L-histidine with D5-Ag NCs as a signal indicator.

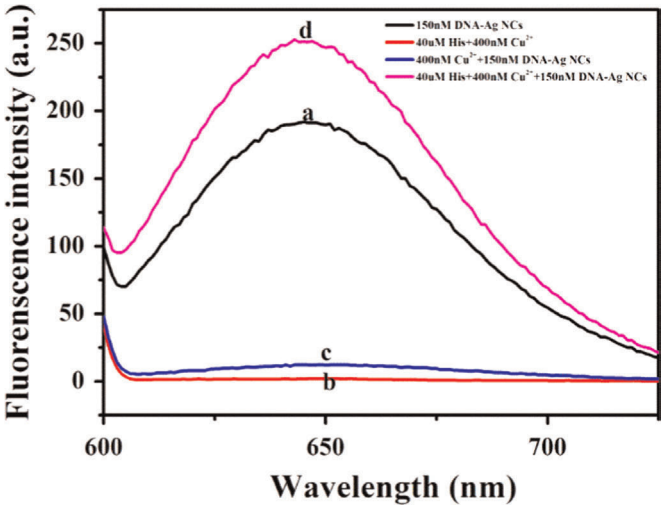

Fig. 1. Emission spectra of (a) 150 nM D5-Ag NCs; (b) 40 μM His+400 nM Cu^{2+}; (c) 400 nM Cu^{2+}+150 nM D5-Ag NCs; (d) 40 μM His+400 nM Cu^{2+}+150 nM D5-Ag NCs. The excitation and emission wavelength are 585 nm and 646 nm, respectively. The concentration and pH value of PB buffer solution were 20 mM and 7.4, respectively.

3.3. Fluorescence quenching of D5-Ag NCs by Cu^{2+}

An optimum concentration of Cu^{2+} in the sensor system (D5-Ag NCs/Cu^{2+}) is an essential prerequisite for the highly sensitive response to L-histidine. If Cu^{2+} was superfluous, more L-histidine was required to interact with Cu^{2+}, and this condition would result in a lower detection limit. On the other hand, if Cu^{2+} was insufficient, the detection of high concentration of L-histidine might not be realized, and that would lead to a narrow detection range. As shown in Fig. 2a and b, with the titration of $Cu(NO_3)_2$ into D5-Ag NCs solution (150 nM, in 20 mM PB buffer, pH 7.4), the instinct fluorescence of D5-Ag NCs (at 650 nm) was gradually quenched, and the quenching of fluorescence through Cu^{2+} could not be affected by the pH value over the range of pH 5.8–8.0 (Zhang et al., 2013c). Because Cu^{2+} could be easily attached to the surfaces of D5-Ag NCs by the coordination with DNA, partial negative charges of DNA would be neutralized and the fluorescence would be effectively quenched via electron or energy transfer (Zhang et al., 2013c). The fluorescence intensity dropped sharply, and then reached a platform. As a result, 88.3% fluorescence intensity of the system was quenched when the concentration of Cu^{2+} was 400 nM, which was used for the following experiments.

3.4. Fluorescence recovery of D5-Ag NCs by L-histidine

To investigate the performance of our strategy for L-histidine detection, different concentrations of L-histidine were added into the mixture of Cu^{2+} and D5-Ag NCs, the fluorescence intensity gradually restored with the increasing concentration of L-histidine (Fig. 3a and b), indicating that the binding ability between Cu^{2+} and the imidazole moiety on L-histidine side chain was stronger than the coordination interaction between Cu^{2+} and D5-Ag NCs. Given that the binding affinity of L-histidine and Cu^{2+} would be more efficient, different concentrations of L-histidine were firstly mixed with Cu^{2+} for 30 min, and then DNA-Ag NCs were added (Fig. S4). The more L-histidine was added, the less Cu^{2+} was left to interact with D5-Ag NCs, the higher fluorescence intensity was observed. When 80 μM L-histidine was added D5-Ag NCs/Cu^{2+} complex, 145% of the D5-Ag NCs fluorescent intensity was restored. More than 100% fluorescence recovery might be observed while additional L-histidine provided better protection from the solvent quenching for D5-Ag NCs. In other words, the D5-Ag NCs should exhibit stronger fluorescence intensity in the presence of the excess of L-histidine (Fig. S5) (Lan et al., 2011b).

As shown in Fig. 4b, a linear relationship was observed over the range of 0.20–80 μM (R^2=0.987) with a detection limit of 4.3 nM based on $3S_0/S$, where S_0 was the standard deviation of background and S was the sensitivity. The relative standard deviation for eleven detections of 10 μM L-histidine was 1.93%, indicating a good repeatability of measurement. For comparison, the detection limits and linear ranges for histidine detection by different sensors were summarized in Table S2. Relative to the other approaches reported (Chen et al., 2014; Elbaz et al., 2008; He et al., 2013, 2012; Kong et al., 2011; Li et al., 2013, 2004; Oliveira et al., 2013; Sun et al., 2012; Zhou et al., 2014), the present strategy does have some advantages, including no chemical modification, high sensitivity, low detection limit and relatively wide detection range.

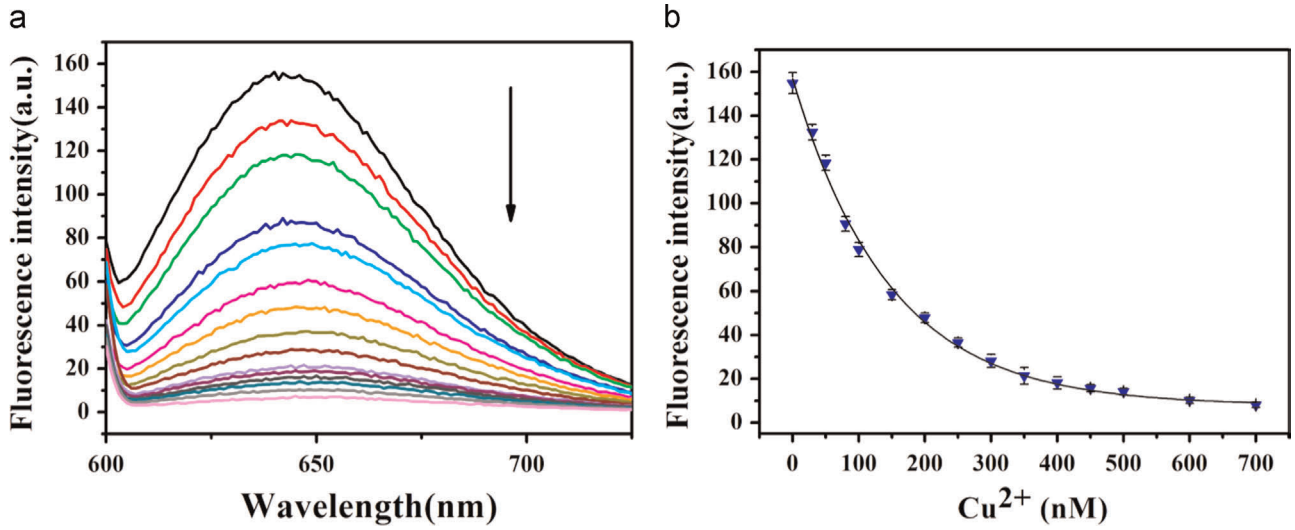

Fig. 2. (a) Fluorescence spectra of the D5-Ag NCs/Cu^{2+} systems (D5-Ag NCs concentration: 150 nM; Cu^{2+} concentration: 0, 30, 50, 80,100, 150, 200, 250, 300, 350, 400, 450, 500, 600 and 700 nM). (b) Fluorescence intensity of D5-Ag NCs against the concentration of Cu^{2+}. The concentration and pH value of PB buffer solution were 20 mM and 7.4, respectively.

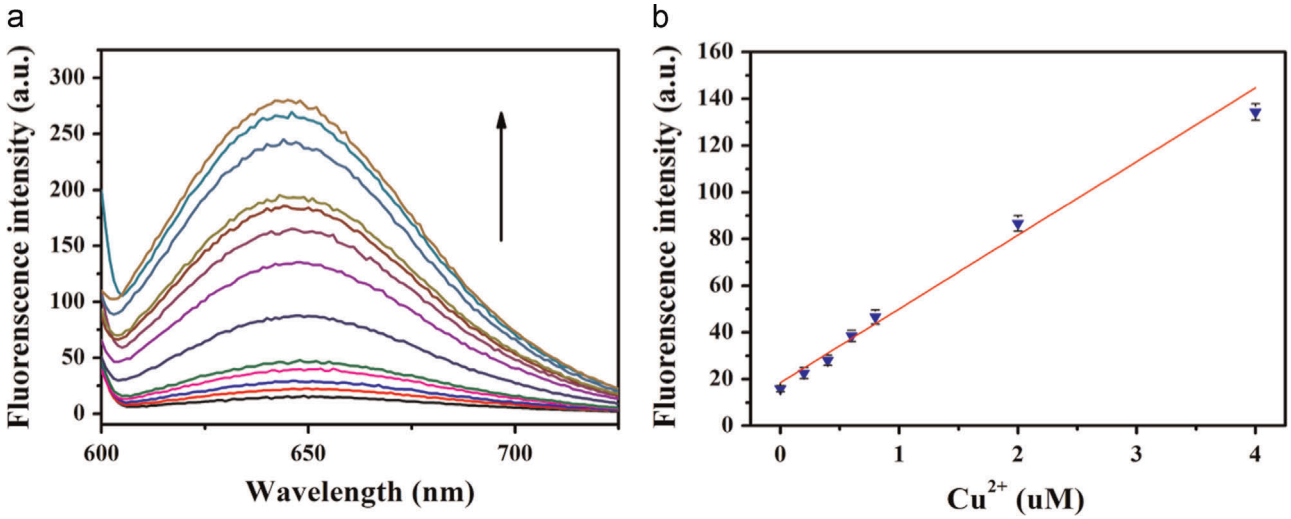

Fig. 3. (a) Fluorescence restoration with the addition of L-histidine (0, 0.2, 0.4, 0.6, 0.8, 1.0, 2.0, 4.0, 6.0, 8.0, 10, 20, 40, 60 and 80 μM) into the D5-Ag NCs/Cu^{2+} system. (b) The linear relationship of the fluorescence intensity of the D5-Ag NCs/Cu^{2+} complex against the concentrations of L-histidine. The concentration and pH value of PB buffer solution were 20 mM and 7.4, respectively.

3.5. Selectivity and competitive assay of fluorescence detection of L-histidine

It is essential to evaluate the selectivity for the sensor strategy developed by us. In addition to the imidazole ring of L-histidine, the thiol group of cysteine can also interact with Cu^{2+}, giving a false positive signal. A masking agent, NEM, was thus introduced into the sensor system by us to eliminate interference of cysteine (He et al., 2013). Consequently, as shown in Fig. 4a, the fluorescence response of the system to L-histidine (10 μM) was more pronounced than those to the other amino acids (20 μM). This result indeed demonstrated that only L-histidine could result in the fluorescence restoration, and the sensor system could selectively discriminate L-histidine from other amino acids. In order to further evaluate the detection selectivity, a competition assay (detecting L-histidine in the presence of the other amino acids) was also performed. Fig. 4b clearly illustrated that the sensor system (D5-Ag NCs/Cu^{2+}) specifically responded to L-histidine, even in the presence of other relevant species. It confirmed that the developed approach did have good selectivity toward L-histidine.

3.6. Detection in human urine

In order to demonstrate the practical application of our fluorescent probe in biological media, 100-fold diluted human urine with 10 mM NEM solution (1:1 volume) samples were used as the medium for further investigations by applying the previous reported methods (Wu and Yan, 2010). The results were summarized in Table 1, with different amount of L-histidine added into the human urine medium, the detected concentration could be obtained through the measurement of the fluorescence intensity of D5-Ag NCs/Cu^{2+} system, and the recovery values could be calculated to be 90%, 95% and 102% for 10 μM, 20 μM and 30 μM of L-histidine, respectively. It suggested that D5-Ag NCs/Cu^{2+} system was rather a promising fluorescence probe for the detection of L-histidine in biological systems.

4. Conclusions

In summary, we have successfully constructed a simple and label-free approach for fluorescent detection of L-histidine based on Cu^{2+} mediated D5-Ag NCs. Under the optimized experimental

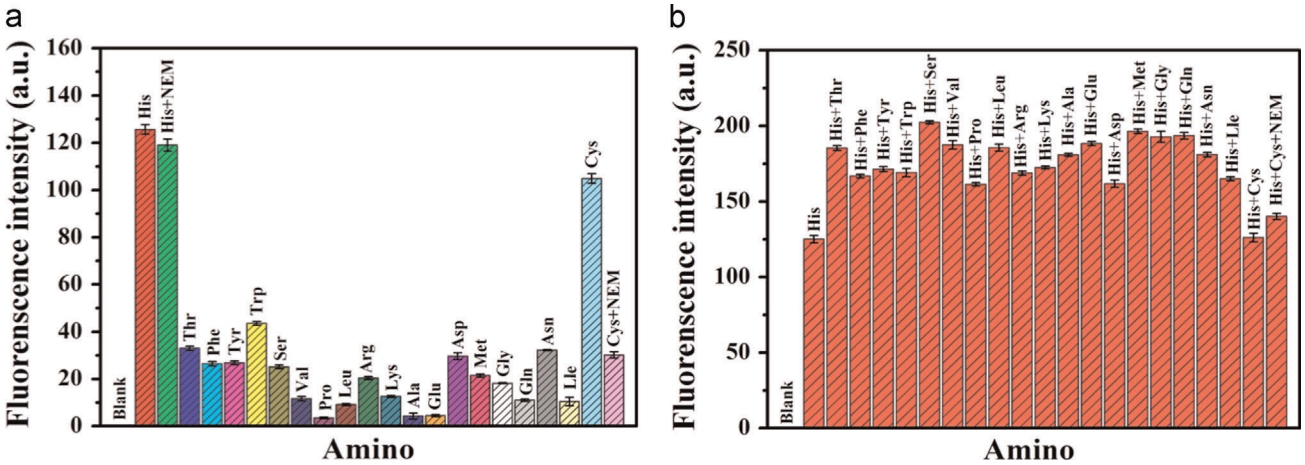

Fig. 4. Selectivity and competitive experiments on the detection of L-histidine against other amino acids. (a) The relative fluorescence intensity of fluorescent probe in the presence 10 μM His against 20 μM other various amino acids. (b) The relative fluorescence intensity of the system upon addition of His (20 μM), and the mixture of His (20 μM) with other various amino acids (20 μM). The concentration and pH value of PB buffer solution were 20 mM and 7.4, respectively.

Table 1
The testing results of different L-histidine concentration in human urine ($N=3$).

Sample no.	Added (μM)	Found (mean ± S.D, μM)	Recovery (%)	R.S.D. (%)
1	10	9.021 ± 0.036	90.21	0.24
2	20	18.962 ± 0.486	94.81	1.48
3	30	30.711 ± 1.383	102.37	2.49

conditions, the protocol offers high selectivity toward L-histidine over other amino acids, including cysteine, with the help of masking agent of NEM. Importantly, the present system can practically applied to detect L-histidine in diluted human urine, exhibiting great opportunities for practical application in biological and clinical diagnosis fields.

Acknowledgments

This work was financially supported by the National Natural Science Foundation of China (81171646, 31170776 and 21472139) as well as by the Fundamental Research Funds for the Central Universities.

Appendix A. Supplementary material

Supplementary data associated with this article can be found in the online version at http://dx.doi.org/10.1016/j.bios.2014.11.013.

References

Ai, J., Guo, W., Li, B., Li, T., Li, D., Wang, E., 2012. Talanta 88, 450–455.
Cao, Y., Shi, S., Wang, L., Yao, J., Yao, T., 2014. Biosens. Bioelectron. 55, 174–179.
Chen, Z., Nai, J., Ma, H., Li, Z., 2014. Electrochim. Acta 116, 258–262.
Chen, Z.B., Mu, X.J., Li, J., Li, L.D., Guo, L., 2012. Adv. Mater. Res. 485, 213–216.
Elbaz, J., Shlyahovsky, B., Willner, I., 2008. Chem. Commun. 13, 1569–1571.
Folmer-Andersen, J.F., Lynch, V.M., Anslyn, E.V., 2005. Chem. Eur. J. 11 (18), 5319–5326.
Fu, T., Zhao, X.H., Bai, H.R., Zhao, Z.L., Hu, R., Kong, R.M., Zhang, X.B., Tan, W., Yu, R. Q., 2013. Chem. Commun. 49 (59), 6644–6646.
Guo, W., Yuan, J., Dong, Q., Wang, E., 2010. J. Am. Chem. Soc. 132 (3), 932–934.
Guo, X., Deng, L., Wang, J., 2013. RSC Adv. 3 (2), 401–407.
Han, B., Wang, E., 2011. Biosens. Bioelectron. 26 (5), 2585–2589.
Han, B., Wang, E., 2012. Anal. Bioanal. Chem. 402 (1), 129–138.
He, H.Z., Wang, M., Chan, D.S., Leung, C.H., Qiu, J.W., Ma, D.L., 2013. Methods 64 (3), 205–211.
He, Y., Wang, X., Zhu, J., Zhong, S., Song, G., 2012. Analyst 137 (17), 4005–4009.
Huang, Z., Du, J., Zhang, J., Yu, X.Q., Pu, L., 2012. Chem. Commun. 48 (28), 3412–3414.
Huang, Z., Pu, F., Lin, Y., Ren, J., Qu, X., 2011. Chem. Commun. 47 (12), 3487–3489.
Kong, R.M., Zhang, X.B., Chen, Z., Meng, H.M., Song, Z.L., Tan, W., Shen, G.L., Yu, R.Q., 2011. Anal. Chem. 83 (20), 7603–7607.
Kundu, S., 2013. Phys. Chem. Chem. Phys. 15 (33), 14107–14119.
Lan, G.Y., Chen, W.Y., Chang, H.T., 2011a. RSC Adv. 1 (5), 802–807.
Lan, G.Y., Chen, W.Y., Chang, H.T., 2011b. Biosens. Bioelectron. 26 (5), 2431–2435.
Lan, G.Y., Huang, C.C., Chang, H.T., 2010. Chem. Commun. 46 (8), 1257–1259.
Li, H., Liu, J., Fang, Y., Qin, Y., Xu, S., Liu, Y., Wang, E., 2013. Biosens. Bioelectron. 41, 563–568.
Li, J., Zhong, X., Cheng, F., Zhang, J.R., Jiang, L.P., Zhu, J.J., 2012a. Anal. Chem. 84 (9), 4140–4146.
Li, J., Zhong, X., Zhang, H., Le, X.C., Zhu, J.J., 2012b. Anal. Chem. 84 (12), 5170–5174.
Li, L.D., Chen, Z.B., Zhao, H.T., Guo, L., 2011. Biosens. Bioelectron. 26 (5), 2781–2785.
Li, X., Ma, H., Nie, L., Sun, M., Xiong, S., 2004. Anal. Chim. Acta 515 (2), 255–260.
Liang, J., Chen, Z., Guo, L., Li, L., 2011. Chem. Commun. 47 (19), 5476–5478.
Liu, J., 2014. Trends Anal. Chem. 58, 99–111.
Liu, J.J., Song, X.R., Wang, Y.W., Zheng, A.X., Chen, G.N., Yang, H.H., 2012. Anal. Chim. Acta 749, 70–74.
Liu, X., Wang, F., Aizen, R., Yehezkeli, O., Willner, I., 2013. J. Am. Chem. Soc. 135 (32), 11832–11839.
Ma, K., Cui, Q., Liu, G., Wu, F., Xu, S., Shao, Y., 2011. Nanotechnology 22 (30), 305502.
Molotsky, T., Tamarin, T., Moshe, A.B., Markovich, G., Kotlyar, A.B., 2010. J. Phys. Chem. C 114 (38), 15951–15954.
Oliveira, E., Santos, C., Poeta, P., Capelo, J.L., Lodeiro, C., 2013. Analyst 138 (13), 3642–3645.
Richards, C.I., Choi, S., Hsiang, J.C., Antoku, Y., Vosch, T., Bongiorno, A., Tzeng, Y.L., Dickson, R.M., 2008. J. Am. Chem. Soc. 130 (15), 5038–5039.
Sakr, M.E., Abou Kana, M.T., Abdel Fattah, G., 2014. Luminescence 29 (7), 938–944.
Shang, L., Dong, S., Nienhaus, G.U., 2011. Nano Today 6 (4), 401–418.
Sharma, J., Rocha, R.C., Phipps, M.L., Yeh, H.-C., Balatsky, K.A., Vu, D.M., Shreve, A.P., Werner, J.H., Martinez, J.S., 2012. Nanoscale 4 (14), 4107–4110.
Sharma, J., Yeh, H.C., Yoo, H., Werner, J.H., Martinez, J.S., 2010. Chem. Commun. 46 (19), 3280–3282.
Sharma, J., Yeh, H.C., Yoo, H., Werner, J.H., Martinez, J.S., 2011. Chem. Commun. 47 (8), 2294–2296.
Sinha, T., Ahmaruzzaman, M., Bhattacharjee, A., 2014. J. Environ. Chem. Eng. 2 (4), 2269–2279.
Sun, S.K., Tu, K.X., Yan, X.P., 2012. Analyst 137 (9), 2124–2128.
Tateda, N., Matsuhisa, K., Hasebe, K., Kitajima, N., Miura, T., 1998. J. Chromatogr. B 718 (2), 235–241.
Wu, P., Yan, X.-P., 2010. Biosens. Bioelectron. 26 (2), 485–490.
Xu, Y.K., Hwang, S., Kim, S., Chen, J.Y., 2014. ACS Appl. Mater. Interfaces 6 (8), 5619–5628.
Yao, J.L., Gao, X., Sun, W., Fan, X.Z., Shi, S., Yao, T.M., 2012. Inorg. Chem. 51 (23), 12591–12593.
Yeh, H.C., Sharma, J., Han, J.J., Martinez, J.S., Werner, J.H., 2010. Nano Lett. 10 (8), 3106–3110.
Yeh, H.C., Sharma, J., Shih Ie, M., Vu, D.M., Martinez, J.S., Werner, J.H., 2012. J. Am. Chem. Soc. 134 (28), 11550–11558.
Yin, J., He, X., Wang, K., Qing, Z., Wu, X., Shi, H., Yang, X., 2012. Nanoscale 4 (1), 110–112.
Yu, X., Wang, Q., 2011. Microchim. Acta 173 (3–4), 293–298.
Zhang, L.-Y., Sun, M.-X., 2004. J. Chromatogr. A 1040 (1), 133–140.
Zhang, L., Wang, E., 2014. Nano Today 9 (1), 132–157.
Zhang, L., Zhu, J., Guo, S., Li, T., Li, J., Wang, E., 2013a. J. Am. Chem. Soc. 135 (7), 2403–2406.
Zhang, L., Zhu, J., Zhou, Z., Guo, S., Li, J., Dong, S., Wang, E., 2013b. Chem. Sci. 4 (10), 4004.
Zhang, L.P., Zhang, X.X., Hu, B., Shen, L.M., Chen, X.W., Wang, J.H., 2012a. Analyst 137 (21), 4974–4980.
Zhang, M., Ye, B.C., 2011. Analyst 136 (24), 5139–5142.
Zhang, P., Wang, Y., Chang, Y., Xiong, Z.H., Huang, C.Z., 2013c. Biosens. Bioelectron. 49, 433–437.
Zhang, S., Yang, C., Zhu, W., Zeng, B., Yang, Y., Xu, Y., Qian, X., 2012b. Org. Biomol. Chem. 10 (8), 1653–1658.
Zheng, J., Nicovich, P.R., Dickson, R.M., 2007. Annu. Rev. Phys. Chem. 58, 409–431.
Zhou, L., Yan, N., Zhang, H., Zhou, X., Pu, Q., Hu, Z., 2010. Talanta 82 (1), 72–77.
Zhou, Y., Zhou, T., Zhang, M., Shi, G., 2014. Analyst 139 (12), 3122–3126.